# Coriolis-Coupled Quantum Dynamics for $O(^1D) + H_2 \rightarrow OH + H$†

**Thomas E. Carroll and Evelyn M. Goldfield***

*Department of Chemistry, Wayne State University, Detroit, Michigan 48202*

*Received: October 16, 2000; In Final Form: December 12, 2000*

The $O(^1D) + H_2 \rightarrow OH + H$ reaction has been studied with a time-dependent wave packet method for total angular momenta $J = 1$, 2, 5, 10, 15, 20, and 30. Total reaction probabilities from calculations in which the Coriolis coupling terms (CC) in the Hamiltonian are included are compared with those from calculations in which the Helicity−Conserving (HC) approximation is employed. The calculations were performed combining a real wave packet method with the Coriolis-coupled method on parallel computers. At low values of *J*, the CC reaction probabilities are somewhat smaller than the HC results; the agreement between the two methods improves, however, as *J* increases. For this reaction, the HC approximation should yield accurate estimates of the reaction cross section and rate constants. However, because reactive collisions involve a high degree of Coriolis mixing, it is very likely that inclusion of these terms will affect calculation of less averaged quantities such as the differential cross section or OH internal energy distributions.

## I. Introduction

The reaction of electronically excited oxygen atoms with hydrogen molecules

$$O(^1D) + H_2 \rightarrow OH + H \qquad (1)$$

has long been of interest to chemical dynamicists and has been the focus of recent experimental[1−4] and theoretical[5−18] work. This system is both complex enough to provide interesting dynamics and simple enough to allow a rather sophisticated theoretical treatment and a significant interplay between theory and experiment.

A recent quantum dynamics study of Gray et al.[6] on reaction 1 focused on the dynamics on the lowest singlet ($\tilde{X}\ ^1A'$) state, which involves the potential energy surface (PES) for the electronic ground state of the water molecule. This work computed reaction probabilities for total angular momentum $J > 0$ using the Helicity−Conserving(HC) approximation, in which Coriolis coupling terms are ignored. Quantum mechanical estimates for the cross section and rate constants were computed using the HC reaction probabilities for $J \leq 15$. A capture model based upon the HC reaction probabilities for some larger value of *J* was used to estimate the contributions to the cross section from $J > 15$. Capture cross section calculations based upon $J = 15$, 20, or 30 all yielded similar results. The study employed two recently developed PES's based on high-quality ab initio data: the "K" PES[16] and the newer surface due to Dobbyn and Knowles.[13]

The quantum capture model cross sections agreed reasonably well with cross sections computed using classical trajectories at two different collision energies, although the quantum cross sections are somewhat lower. Since the classical studies include Coriolis coupling and the quantum studies do not, the question is raised as to whether the Coriolis terms are in fact important for this reaction. Recent quantum dynamics studies on another complex-forming reaction

$$H + O_2 \rightarrow OH + O \qquad (2)$$

have shown that, in fact, including Coriolis coupling terms in the Hamiltonian is crucial for an accurate description of the dynamics of that reaction.

The present study addresses the role of Coriolis coupling in reaction 1 by carrying out fully coupled quantum dynamics (CC) for select values of *J* and comparing with their Helicity−Conserving (HC) counterparts. Gray et al.[6] noted that the reaction probabilities exhibit different types of behavior for low, intermediate, and high values of *J*. We explore the effect of Coriolis coupling on each of these *J* limits. The organization of the paper is as follows. In section II, we present the theory. Section III gives the computational details. In section IV, we present results for the reaction probabilities as a function of energy and total angular momentum. In section V, we discuss the implications of our results.

## II. Theory

The computational method and the computer programs employed are similar to those used in previous calculations by Meijer and Goldfield on the $H + O_2$ reaction.[19−21]

**A. Coordinates and Basis Set.** We use the standard body-fixed (BF) Jacobi coordinates *R*, *r*, and $\vartheta$, which are the length of the distance vector **R** between O and the center-of-mass of $H_2$, the length of the $H_2$ internuclear distance **r**, and the angle between **R** and **r**, respectively. The overall rotation of the complex with respect to a space-fixed (SF) coordinate system is given by three Euler angles, collectively denoted by $\boldsymbol{\alpha}$.

Good quantum numbers are the total angular momentum quantum number, *J*, the projection of **J** onto the SF *z*-axis, *M*, and the parity of the wave function under inversion of the SF nuclear coordinates, *p*. We expand the wave function as a function of these quantum numbers. We use a sinc-DVR[22] with "wrapped" basis functions[23] $\phi_\lambda^-(R)$ and $\phi_\nu^-(r)$ for the *R* and *r* coordinates, respectively.

For the angular coordinate, as in previous work,[19−21] we employ a basis of parity-adapted angular basis functions, $G_{j\Omega}^{J,M,p}(\boldsymbol{\alpha},\vartheta)$. Here, *j* is the rotational angular momentum of $H_2$

† Part of the special issue "Aron Kuppermann Festschrift".

* Corresponding author. E-mail: evi@sun.science.wayne.edu.

10.1021/jp0037854 CCC: $20.00 
Published on Web 01/27/2001

and $\Omega$ is the projection of both **j** and **J** on **R**. The basis functions $G^{J,M,p}_{j\Omega}(\alpha,\vartheta)$ are defined as

$$G^{J,M,p}_{j\Omega}(\alpha,\vartheta) = [2(1+\delta_{\Omega,0})]^{1/2}\,\Theta^{\Omega}_{j}(\vartheta)[F^{J}_{\Omega M}(\alpha) + (-1)^{J+\Omega+p}\,F^{J}_{-\Omega M}(\alpha)] \quad (3)$$

$\Theta^{\Omega}_{j}(\vartheta)$'s are associated Legendre functions in the phase convention of Condon and Shortley.[24] $F^{J}_{\Omega M}(\alpha)$'s are normalized Wigner D-matrixes.[25,26]

This results in the following expression for the wave functions $\Psi^{J,M,p}$:

$$\Psi^{J,M,p}(R,r,\alpha,\vartheta;t) = \sum_{\Omega=\Omega_{\min}}^{J}\sum_{j\geq\Omega}^{j_{\max}}\sum_{\nu=1}^{N_R}\sum_{\lambda=1}^{N_R} C^{J,M,p}_{\lambda\nu j\Omega}(t)\phi^{-}_{\lambda}(R)\phi^{-}_{\nu}(r)G^{J,M,p}_{j\Omega}(\alpha,\vartheta) \quad (4)$$

$\Omega_{\min}$ is equal to 0 or 1, depending on the spectroscopic parity[27,28] $(-1)^{J+p}$.

In this study, we consider reactions from $H_2$ in its ground rovibrational state, ($v_i = 0, j_i = 0$). Therefore, the only allowed value for $\Omega$ in the reactant asymptote is $\Omega = 0$, which means that we confine ourselves to even values of the spectroscopic parity. Due to the exchange symmetry of $H_2$ we need to include only even values of $j$ in the basis set expansion.

**B. Hamiltonian, Propagation, and Analysis.** The triatomic Hamiltonian in Jacobi coordinates for the $O(^1D) + H_2$ system in the BF frame is given by

$$\hat{H} = -\frac{\hbar^2}{2\mu_R}\frac{\partial^2}{\partial R^2} - \frac{\hbar^2}{2\mu_r}\frac{\partial^2}{\partial r^2} + \frac{(\hat{J}-\hat{j})^2}{2\mu_R R^2} + \frac{\hat{j}^2}{2\mu_r r^2} + V(R,r,\vartheta) \quad (5)$$

where $\mu_R$ and $\mu_r$ are the reduced mass of the $O + H_2$ collision complex and the reduced mass of $H_2$, respectively. $V(R,r,\vartheta)$ is the intermolecular potential, which in this case is the "K" PES of Ho et al.[16]

Using the basis set expansion, given in eq 4, we derived the equations of motion given in detail in ref 21. The equations of motion are tridiagonal in the projection quantum number $\Omega$: all terms are diagonal in $\Omega$ except for the Coriolis terms, which couple $\Omega$ to $\Omega \pm 1$.

For computational efficiency, we employ the real wave packet propagation scheme of Gray and Balint-Kurti.[29] In this method, the Hamiltonian in eq 5 is represented by a finite, real matrix **H**, and the wave packet $\Psi$ is represented by a real finite vector **q**. Similar methods have been developed by Kouri and coworkers,[30,31] Mandelshtam and Taylor,[32,33] Kroes and Neuhauser,[34] and Chen and Guo.[35,36] The method is based upon the fact that reaction probabilities pertinent to a Hamiltonian operator may be inferred from a wave packet which has evolved under a modified time-dependent Schrödinger equation in which the Hamiltonian operator has been replaced by a function of itself, $f(\hat{H})$.[29,37] In fact, one may choose $f(\hat{H})$ so that the act of propagating forward one time step is accomplished by a simple Chebyshev iteration involving a single evaluation of the Hamiltonian on a real vector

$$\mathbf{q}_{k+1} = \mathbf{A}\cdot(-\mathbf{A}\mathbf{q}_{k-1} + 2\mathbf{H}_s\mathbf{q}_k) \quad (6)$$

where $\mathbf{H}_s = a_s\mathbf{H} + b_s$. $a_s$ and $b_s$ are chosen in such a way that all eigenvalues of $\mathbf{H}_s$ lie between $-1$ and 1. The matrix **A** ensures that the wave packet is absorbed at the edge of the grid to avoid reflections. **A** is defined as the matrix representation of the operators $A^R_\lambda$ and $A^r_\nu$, where $A^R_\lambda = 1$ for $R \leq R_{abs}$ and $A^R_\lambda = \exp[-B_R(R_\lambda - R_{abs})^2]$ for $R \geq R_{abs}$. A similar definition holds for $A^r_\nu$. The absorption parameters are given in Table 1

**TABLE 1: Parameters for the Calculation**

| quantity | value |
|---|---|
| $\beta$ | 0.08 au |
| $k_0$ | 4.23 (6.26) au[a] |
| $R_0$ | 7.5 (12)au[b] |
| $R_{\min}$ | 0.0 au |
| $R_{\max}$ | 14.5 (17.5) au |
| $N_R$ | 209 (251) |
| $r_{\min}$ | 0.5 au |
| $r_{\max}$ | 11.5 au |
| $N_r$ | 127 |
| $V^{(o)}_{\text{cut}}$ | 2.3 eV |
| $V^{(i)}_{\text{cut}}$ | 8.16 eV |
| $V_{\text{cut}}$ | 12.2 eV |
| $j_{\max}$ | 89 (even $j$'s only) |
| $B_R$ | 0.0005 au |
| $R_{\text{abs}}$ | 9.5 (13.3) au |
| $B_r$ | 0.0002 au |
| $r_{\text{abs}}$ | 6.5 au |
| $R_s$ | 9.18 (12.94 au) |
| $r_s$ | 5.41 au |

[a] For $J > 10$, convergence over the entire energy range required propgations of a "low" and "higher" energy wave packet. [b] Quantities in parentheses are for $J \geq 10$.

To reduce the amount of memory that the calculations require, we transform from the associated Legendre basis or finite basis representation (FBR) to a grid or discrete variable representation (DVR) in $\vartheta$ to compute the action of the potential energy operator, **V**.[38] In the DVR representation, the potential energy matrix **V** is diagonal, whereas the FBR representation requires a reduced potential matrix $\mathbf{V}^{\Omega}_{jj'}$, with elements given by $\langle\Theta^{\Omega}_{j}|V|\Theta^{\Omega}_{j'}\rangle$. Just as the symmetry of the hydrogen molecule allows us to use only even $j$ states in the Legendre expansion, it also allows us to use only half of the Gauss−Legendre grid points in the DVR representation.[39] We have implemented this transformation so that it does not require more CPU time than the more straightforward FBR approach. We use a recently developed flux-based approach for extracting the energy-dependent reaction probabilities from the real wave packets.[37] To obtain probabilities for both reaction, $P^J_R(E)$, and nonreaction, $P^J_{NR}(E)$, we compute the flux through dividing surfaces at large values of both $R = R_s$ and $r = r_s$. The values for these parameters are given in Table 1.

**C. Parallel Method.** The tridiagonal form for the equations of motion forms the basis of the parallel method we use to facilitate our calculations. For smaller $J$ states, it is appropriate to use the straightforward method of assigning blocks of the wave function corresponding to a particular $\Omega$ to a specific processor on a parallel machine.[40] For large $J$ states, it is much more efficient to assign two $\Omega$ states to each processor in such a way that the load on each processor is nearly the same. To accomplish this, we use the wrapping method described in ref 40. This method takes into account the fact that for each $\Omega$ state, $j \geq \Omega$, so that the size of the rotational basis decreases as $\Omega$ increases. Consider, for example, the even (spectroscopic) parity, $J = 7$ case using four processors. We assign the blocks corresponding to the different $\Omega$ states as follows: $\Omega = 0, 7 \rightarrow$ processor 0; $\Omega = 1, 6 \rightarrow$ processor 1; $\Omega = 2, 5 \rightarrow$ processor 2; and $\Omega = 3, 4 \rightarrow$ processor 3. For an odd number of $\Omega$ states, the problem is a bit more difficult, but generally the first processor is singled out and assigned only one $\Omega$ state (either $\Omega = 0$ or $\Omega = 1$, depending on the parity) as well as I/O and

other serial tasks. The only communication between the processors arises from calculating the Coriolis terms, and is small compared to, e.g., the calculation of the vibrational terms in the equations of motion.[21,40] In our calculations, we use MPI[41−43] to perform the communication between the processors (see refs 21 and 40 for more details). Use of the "wrapping method", with two Ω's per processor was made possible by the substantial savings in memory usage through switching to the FBR-DVR approach (see section IIB). Because of memory considerations, we have not been able place more than two Ω states on a processor. The method easily generalizes, however, to any even number of Ω states per processor.

**D. Initial Conditions.** In all calculations, we take $j_i = 0$ and $v_i = 0$, where $j_i$ is the initial rotational angular momentum quantum number of $H_2$ and $v_i$ its initial vibrational angular momentum. An incoming Gaussian wave packet is used to describe the initial state in the entrance channel

$$G(R) = \frac{1}{\sqrt[4]{2\pi\beta}} \exp(-ik_0R) \exp\left[\frac{-(R - R_0)^2}{4\beta}\right] \qquad (7)$$

where $R_0$ is the center of the wave packet and $k_0\hbar$ is a linear momentum. The parameters used in eq 7 are given in Table 1.

To initiate the Chebyshev expansion, we use the method described in ref 6. To begin the iteration in eq 6 above, we requre $\mathbf{q_0}$ and $\mathbf{q_1}$. We take $\mathbf{q_0}$ to simply be the real part of the complex initial wave packet. Since the initial condition is complex, $\mathbf{q_1}$ must be evaluated according to $\mathbf{q_1} = \mathbf{H_s}\cdot\mathbf{q_0} - (1 - \mathbf{H_s}^2)^{1/2}\cdot\mathbf{p_0}$, where $\mathbf{p_0}$ is the imaginary part of the initial condition.[29] The square root operator is also expanded in terms of Chebyshev polynomials. Usually, 200 polynomials are sufficient to converge this expansion.

## III. Computational Details

The parameters used in the calculation are all given in Table 1. Note that three different values for the potential cut off are given. The reduced potential is cut off at $V_{cut}$, whereas $V_{cut}^{(o)}$ and $V_{cut}^{(i)}$ refer to parameters used in our program to reduce the size of the grid. This method is described in detail in ref 21.

We propagated the wave packets for 30 000−40 000 Chebyshev iterations such that $P_{tot}^J = P_R^J(E) + P_{NR}^J(E)$ does not deviate from 1 by more than $10^{-2}$ over the energy range of interest except for very low collision energies. The typical deviation is $<10^{-3}$. For $J > 10$, we found it necessary to run two wave packets, with two values of $k_0$ to obtain good convergence at lower and higher energies. It can be difficult to obtain convergence at very low energies, and for some values of $J$, we were not able to obtain satisfactory results below 0.008 eV collision energy. For high $J$ states, although we obtain an excellent description of the $P_R^J$ in the centrifugal barrier region, $P_{NR}^J$ is not so well described, so in this region $P_{tot}^J$ deviates considerably from 1.

A Helicity−Conserving (single processor) $J = 20$ run took 1.13 h wall-clock time for 1000 iterations on the IBM SP at NERSC running on dedicated nodes. A comparable $J = 20$ Coriolis-coupled run on 21 processors took 1.39 h. Since a HC run uses 40 $O_2$ rotational basis states whereas a CC calculation requires 740 such states, the CC job performs roughly 18.5 times more work than the HC job. We can get an estimate of how well the job scales with size, by computing the efficiency, $E_f$ of the parallel program through the formula

$$E_f = \frac{\text{increase in work}}{\text{number of processors}} \times \frac{\text{time for a single processor job}}{\text{time for the CC job}} \qquad (8)$$

Using eq 8, we obtain $E_f = 0.71$. (The ideal value for $E_f$ is 1.)

Of course, since the Coriolis terms must all be computed at each iteration before the computation can proceed, the efficiency of the job is limited by the processor that must complete the largest amount of work. The one Ω per processor model has no way of taking advantage of the fact that there are smaller numbers of basis functions for larger Ω states. The "wrapped calculations", however, do take advantage of this, by attempting to balance out the load on most of the processors. The "wrapped" $J = 20$ run used 11 processors, with 2 Ω states on 10 of them. This job took 2.46 h for 1000 iterations. The efficiency is somewhat greater for this run: $E_f = 0.77$. In general, the advantages of wrapping increase sharply as $J$ increases. One very large practical advantage of "wrapping" the large $J$ calculations is that at most facilities, the fewer the processors you request, the faster the job is scheduled to run.

## Results

In Figure 1, we present reaction probabilities, $P_R^J(E)$ as a function of collision energy for $J$ equal to 1, 2, 5, 10, 15, 20, and 30. Each of the plots shows the Coriolis-coupled (CC) and Helicity−Conserving (HC) results. All of the results shown were computed for this work. Wherever comparison is possible, however, our HC results are in excellent agreement with those of Gray et al.[6]

Following Gray et al.,[6] we group our results into low, intermediate, and high values of $J$ with different limiting behavior. We discuss the effects of including Coriolis terms on each of these different groups. We shall see these effects are very different within each of the different groupings.

**A. $J = 1$: Low $J$.** In stark contrast to the $H + O_2$ reaction, it is in the low $J$ limit that the Coriolis terms have the most pronounced effect for reaction 1. Both the CC and the HC reaction probabilities are highly structured, indicating the presense of somewhat long-lived collision complexes. The main effect of including the Coriolis terms is to lower the reaction probability for some values of the collision energy. In fact, for collision energies ≤ 0.72 eV, the average value of $P_R^{J=1}(E)$ is 0.76 (CC) and 0.82 (HC).

**B. $J = 2$, 5, and 10: Intermediate $J$.** In this region, we see a transition to from low $J$ to high $J$ behavior. Because the centrifugal barrier effects are not significant for $J < 15$, these intermediate partial waves will contribute to the reaction cross section at all collision energies. As $J$ increases, the reaction probability also increases, attaining typical values of 0.92−0.96 at all collision energies except for those very near zero collision energy. The $J = 2$,5 reaction profiles have some features in common with the low $J$ results: there is still significant resonance structure in both the CC and the HC results, and the Coriolis terms serve to lower the reaction probability somewhat. For $J = 10$, however, the situation is quite different. The main differences between the CC and the HC reaction probabilities is that the CC results are much smoother and tend to be higher than the HC results.

**C. $J = 15$, 20, and 30: High $J$.** The level of agreement between the CC and the HC reaction probabilities in the higher $J$ regime appears to be quite good. While there are some differences, particularly for $J = 30$ where the error in the HC results can be as high as 10%, the main effect of the Coriolis

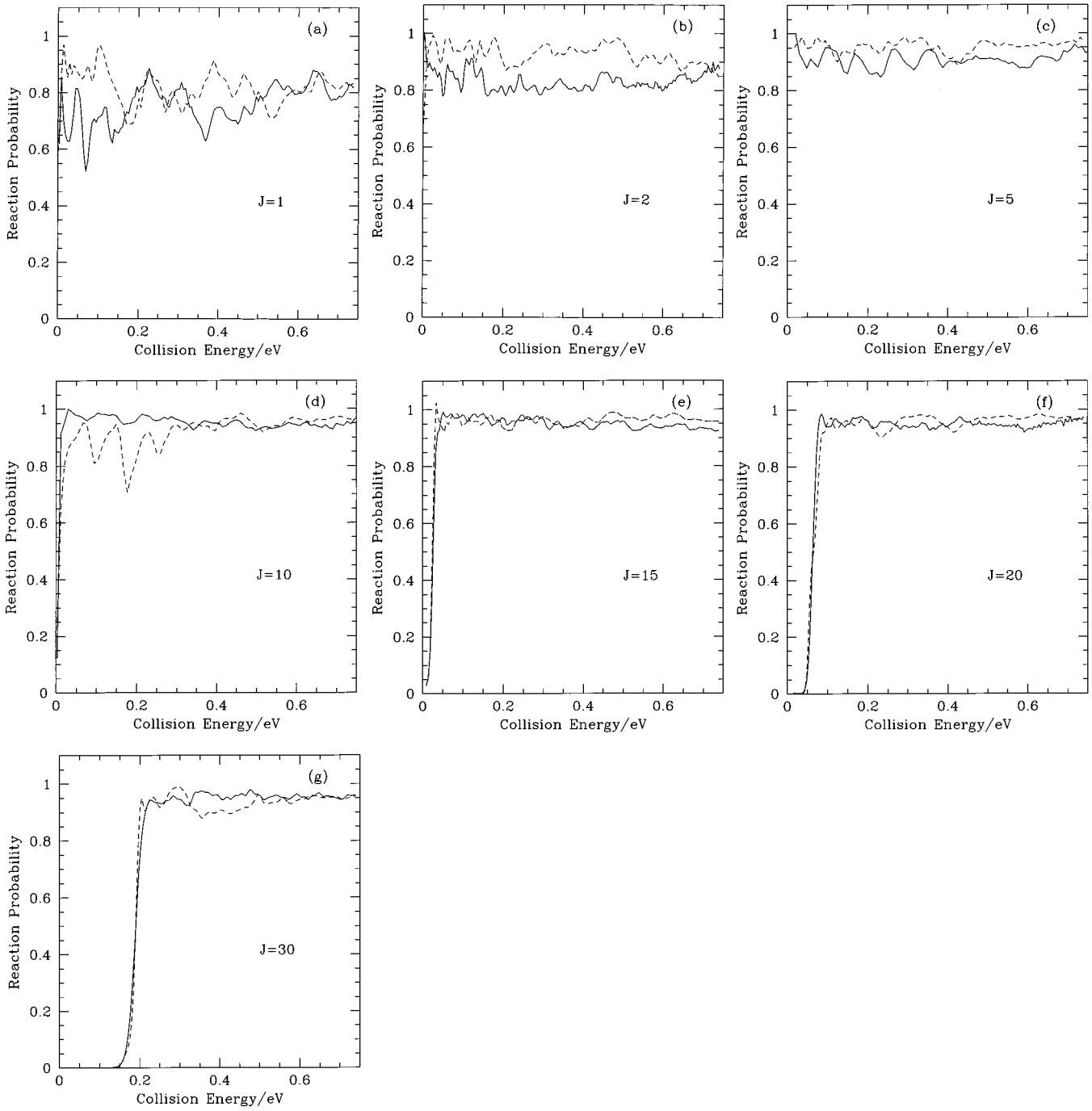


**Figure 1.** Total reaction probability for several values of *J*. Solid line: Coriolis-coupled results. Dashed line: Helicity conserving results.

terms is to smooth out resonance structure. The CC reaction probabilities are not, on average, lower than the HC ones.

## V. Discussion

As discussed in ref 6, the low *J* reaction probabilities are considerably lower than those at higher *J* states which are close to unity. A simple explanation[6] is that, because the minimum energy path for this reaction corresponds to O approaching $H_2$ along its perpendicular bisector, low impact parameter (low *J*) collisions tend to excite the symmetric stretch. For reaction to occur, however, the symmetry must be broken. Higher *J* collisions favor excitation of the antisymmetric stretch and bending modes of the $H_2$ O complex, facilitating the formation of OH + H.

One of the most interesting aspects of the results shown above is that even in the HC approximation, there is much less resonance structure at high *J* collisions than at low *J* collisions. Because only $\Omega = 0$ is included in the HC calculations, this lack of resonance structure cannot be a result of averaging over $\Omega$'s. This smoothing out of resonance structure could indicate that the lifetime of the collision complex decrease as *J* increases, so that in the high *J* regime, $P_R^J(E)$ consists of broad, overlapping resonances. This idea is consistent with the general rise in $P_R^J(E)$ as *J* increases. Consider two limiting cases: a long-lived complex versus a direct insertion process where the H−H bond opens up and the oxygen atom simply passes through carrying off one of the H atoms. While a long-lived complex will have a chance of dissociating back to reactants, a direct insertion

will always be reactive. These ideas are borne out by classical trajectory calculations. At a collision energy of 0.5 kcal/mol Schatz[44] examined the lifetime of collision complexes as a function of impact parameter, *b*, and saw an unmistakable trend toward decreasing lifetime as *b* increases. The number of time steps inside the complex goes down linearly with *b*, corresponding to a lifetime of 90 fs for $b = 0-50$ fs for $b = 6$. Above $b = 6$, the time is roughly constant to $b = 7$, and then it drops precipitously to zero at 7.8, corresponding to when the centrifugal energy is so high that complexes are no longer formed.

The effect of the Coriolis terms is different in the two regimes: in the low *J* regime, the effect is to lower reaction probability for most energies while at high *J*, the main effect is to further smooth out the remaining resonance structure. It is important to note that for the reactive collisions, many $\Omega$ states are highly populated, and all make a significant contribution. For example, for $J = 10$ at a collision energy of.13 eV, only 17% of the reaction probability comes from $\Omega = 0$ and only 30% from $\Omega = 0$ and 1 combined, with 4.5% coming from $\Omega = 10$. For $J = 20$, at 0.13 eV, only 9% of the total raction probablility comes from $\Omega = 0$ and only 30% from $\Omega = 0$, 1, and 2 combined, with about 6% coming from $\Omega \geq 15$. It is very likely that the transitions between $\Omega$ components occur in the interaction region and in the exit channel.

In the CC calculations, for high *J* regimes, the reaction profile of any one $\Omega$ contribution, will show more resonance structure than the total reaction probability and more than the HC reaction profile for that *J*. The contribution of many $\Omega$ components, each with a somewhat different reaction profile and resonance structure, to the reaction probability leads to a general smoothing of the $P_E^J(E)$ plots at higher J. On the basis of these profiles alone, one might be tempted to attribute the relative smoothness of the high *J* reaction profiles solely to the inhomogeneous broadening due to the contribution of the various $\Omega$ components. The relative smoothness of the HC reaction profiles with only one $\Omega$ component, however, indicates that both inhomogeneous broadening and shorter resonance lifetimes may be playing a role as *J* increases. In this regime of broad overlapping resonances and high reaction probabliity across the energy spectrum, it is not possible to say which mechanism is more important based on the structure of the total reaction probabilities.

In the case of low *J*, i.e., $J = 1$, the $\Omega = 0$ component dominates $P_R^{J=1}(E)$ in the CC calculations, and there is no significant smoothing due to inhomogeneous broadening effects.

In contrast to the reaction probability at high *J* regimes, 61% of the nonreactive probability comes from $\Omega = 0$ and 88% from $\Omega = 0$ and 1 combined. Since $\Omega > 0$ can only come from states with $j > 0$, the $\Omega > 0$ contribution to the nonreactive channel arises from inelastic scattering processes in which the rotation of the $O_2$ is excited.

Why the reaction probability at low "J" is lowered when Coriolis terms are included is not as easy to understand. At first glance, it seems to be a bit puzzling because it is only reactive collisions that populate higher $\Omega$ states to any significant extent. But most of these $\Omega \leftrightarrow \Omega \pm 1$ transitions occur after the commitment to reaction has been made, including in the exit channel, and will have no effect on the reaction probability. The answer is probably related to the need for excitation of the antisymmetric stretch and bending modes for reaction to occur. Using a simple classical model, $\Omega = 0$ motion corresponds to rotation of the $H_2$ in the molecular plane, which will enhance the asymmetric stretching mode necessary for reaction. Contributions from higher $\Omega$ components, however, represent out-of-plane bending and will be less effective in promoting excitation of this mode.

Because of the $2J + 1$ degeneracy factor, observables such as the reaction cross sections or rate constants will be dominated by the states with the highest *J* values which contribute to reaction at a given energy. The maximum *J* that contributes to the cross section for a particular energy will be determined by centrifugal barrier effects. But for the "K" potential, centrifugal barrier effects do not really come into play until $J = 15$ (see Figure 4 in ref 6). Therefore, even at low collision energies, $J \approx 15$ will dominate the cross section. Since the HC approximation works well at high *J* collisions, it should be quite suitable for computing these quantities. It would be reasonable, however, to test the suitability of the HC approximation for the initial $j > 0$, where more than one initial $\Omega$ contributes to the process.

Because of some differences in the resonance structure for the HC and the CC methods and because Coriolis coupling does lead to high populations for the $\Omega > 0$ states, the HC approximation may not work so well for less averaged quantities such as product distributions or differential cross sections. For example, the rotational or vibrational distribution of the OH resulting from in-plane rotation of the $H_2$ might be quite different from the rotational or vibrational distribution resulting from out-of-plane rotation. There is another complication regarding using the HC approximation to compute the OH product distributions or differential cross sections. The HC approximation depends both on the coordinate system and the body-fixed *z* axis chosen for the calculation. The reactant coordinates used in this study are not the most suitable for computing product distributions; product coordinates might be much better. But the initial state, $H_2(v_i = 0, j = 0, \Omega = 0)$ is defined in relation to the reactant coordinate system with *R* as the reference axis. A description of this initial state in terms of product coordinates will involve all projections of angular momentum, $\Omega'$, on the reference axis in product coordinates. In this case, ignoring the Coriolis terms will not save much in terms of work but may be quite costly in terms of accuracy (see the discussion in ref 20). Therefore, it is desirable to use a rigorous treatment of angular momentum when computing these quantities.

**Acknowledgment.** We would like to thank Stephen Gray, George Schatz, and Anthony Meijer for useful discussions. We also thank George Schatz for providing the results of trajectory calculations. E.M.G. acknowledges support for this research from NSF Grant CHE-9970994. We also acknowledge generous grants of computer time from the Argonne High Performance Computing Research Facility and the Wayne State High Performance Computing Facility. This research also used resources of the National Energy Research Scientific Computing Center, which is supported by the Office of Science of the U.S. Department of Energy under Contract DE-AC03-76SF00098.

## References and Notes

(1) Liu, X. H.; Lin, J. J.; Harich, S.; Schatz, G. C.; Yang, X. M. *Science* **2000**, *289*, 5484.

(2) Hsu, Y.-T.; Wang, J.-H.; Liu, K. *J. Chem. Phys.* **1997**, *107*, 2351.

(3) Alexander, A. J.; Blunt, D. A.; Brouard, M.; Simons, J. P.; Aoiz, F. J.; Banares, L.; Fujimara, Y. *Faraday Discuss.* **1997**, *108*, 375.

(4) Alagia, M. A.; Balucani, N.; Cartechini, L.; Casavecchia, P.; van Kleef, E. H.; Volpi, G. G.; Kuntz, P. J.; Sloan, J. J. *J. Chem. Phys.* **1998**, *108*, 6698.

(5) Gray, S. K.; Balint-Kurti, G. G.; Schatz, G. C.; Lin, J. J.; Liu, X.; Harich, S.; Yang, X. *J. Chem. Phys.* **2000**, *113*, 7330.

(6) Gray, S. K.; Goldfield, E. M.; Schatz, G. C.; Balint-Kurti, G. G. *Phys. Chem. Chem. Phys.* **1999**, *1*, 1141.

(7) Balint-Kurti, G. G.; Gonzales, A. I.; Gray, S. K.; Goldfield, E. M. *Faraday Discuss.* **1998**, *110*, 169.
(8) Aoiz, F. J.; Banares, L.; Brouard, M.; Castillo, J. F.; Herrero, V. J. *J. Chem. Phys.* **2000**, *113*, 5339.
(9) Aoiz, F. J. *Faraday Discuss.* **1998**, *110*, 245.
(10) Aoiz, F. J.; Banares, L.; Herrero, V. J. *J. Chem. Soc., Faraday Trans.* **1998**, *94*, 2483.
(11) Schatz, G. C.; Pedersen, L. A.; Harding, L. B.; Kuntz, P. J. *Faraday Discuss.* **1998**, *108*, 357.
(12) Schatz, G. C.; Papaioannou, A.; Pedersen, L. A.; Harding, L. B.; Hollebeek, T.; Ho, T.-S.; Rabitz, H. *J. Chem. Phys.* **1997**, *107*, 2340.
(13) Dobbyn, A. J.; Knowles, P. J. *Faraday Discuss.* **1998**, *110*, 247.
(14) Varandas, A. J. C.; Voronin, A. I.; Riganelli, A.; Caridade, P. J. S. B. *Chem. Phys. Lett.* **1997**, *278*, 325.
(15) Dai, J. *J. Chem. Phys.* **1997**, *197*, 4934.
(16) Ho, T.-S.; Hollebeek, T.; Rabitz, H.; Harding, L. B.; Schatz, G. C. *J. Chem. Phys.* **1996**, *105*, 10472.
(17) Peng, T.; Zhang, D.-H.; Zhang, J. Z. H.; Schinke, R. *Chem. Phys. Lett.* **1996**, *248*, 37.
(18) Hankel, M.; Balint-Kurti, G. G.; Gray, S. K. *J. Chem. Phys.* **2000**, *113*, 9658.
(19) Goldfield, E. M.; Meijer, A. J. H. M. *J. Chem. Phys.* **2000**, *113*, 11055.
(20) Meijer, A. J. H. M.; Goldfield, E. M. *J. Chem. Phys.* **1999**, *110*, 870.
(21) Meijer, A. J. H. M.; Goldfield, E. M. *J. Chem. Phys.* **1998**, *108*, 5404.
(22) Colbert, D. T.; Miller, W. H. *J. Chem. Phys.* **1992**, *96*, 1982.
(23) Groenenboom, G. C.; Colbert, D. T. *J. Chem. Phys.* **1993**, *99*, 9681.
(24) Condon, E. U.; Shortley, G. H. *The Theory of Atomic Spectra*; Cambridge University Press: Cambridge, U.K., 1935.
(25) T Pack, R.; Parker, G. A. *J. Chem. Phys.* **1987**, *87*, 3888.
(26) Rose, M. E. *Elementary Theory of Angular Momentum*; Wiley: New York, ***1957***.
(27) Brown, J. M.; Hougen, J. T.; Huber, K.-P.; Johns, J. W. C.; Kopp, I.; Lefebvre-Brion, H.; Merer, A. J.; Ramsay, D. A.; Rostas, J.; Zare, R. N. *J. Mol. Spectrosc.* **1975**, *55*, 500.
(28) van der Avoird, A.; Wormer, P. E. S.; Moszyński, R. *Chem. Rev.* **1994**, *94*, 1931.
(29) Gray, S. K.; Balint-Kurti, G. G. *J. Chem. Phys.* **1998**, *108*, 950.
(30) Huang, Y.; Kouri, D. J.; Hoffman, D. K. *J. Chem. Phys.* **1994**, *101*, 10493.
(31) Huang, Y.; Iyengar, S. S.; Kouri, D. J.; Hoffman, D. K. *J. Chem. Phys.* **1996**, *105*, 927.
(32) Mandelshtam, V. A.; Taylor, H. S. *J. Chem. Phys.* **1995**, *102*, 7390.
(33) Mandelshtam, V. A.; Taylor, H. S. *J. Chem. Phys.* **1995**, *103*, 2903.
(34) Kroes, G.-J.; Neuhauser, D. *J. Chem. Phys.* **1996**, *105*, 8690.
(35) Chen, R.; Guo, H. *Chem. Phys. Lett.* **1996**, *261*, 605.
(36) Chen, R.; Guo, H. *J. Chem. Phys.* **1996**, *105*, 3569.
(37) Meijer, A. J. H. M.; Goldfield, E. M.; Gray, S.; Balint-Kurti, G. G. *Chem. Phys. Lett.* **1998**, *293*, 270.
(38) Choi, S. E.; Light, J. C. *J. Chem. Phys.* **1989**, *90*, 2593.
(39) Whitnell, R. M.; Light, J. C. *J. Chem. Phys.* **1989**, *89*, 3674.
(40) Goldfield, E. M.; Gray, S. K. *Comput. Phys. Commun.* **1996**, *98*, 1.
(41) Gropp, W.; Lusk, E.; Skjellum, A. *Using MPI: Portable Parallel Programming with the Message-Passing Interface*; MIT Press: Cambridge, MA, 1994.
(42) Snir, M.; Otto, S. W.; Huss-Ledermann, S.; Walker, D. W.; Dongarra, J. *MPI: The Complete Reference*; MIT Press: Cambridge, MA, 1994.
(43) See also: http://www.mcs.anl.gov/mpi and http://www.mcs.anl.gov/mpi/mpich.
(44) Schatz, G. C. Private communication.